PAN
POLISH ACADEMY OF SCIENCES

Opto-Electronics Review

journal homepage: https://journals.pan.pl/opelre

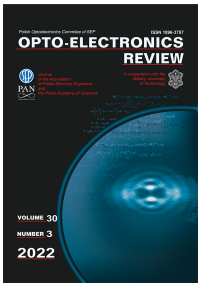

The Al_2O_3/TiO_2 double antireflection coating deposited by ALD method

Marek Szindler[a*], Magdalena M. Szindler[b], Justyna Orwat[c], Grażyna Kulesza-Matlak[d]

[a] Scientific and Didactic Laboratory of Nanotechnology and Material Technologies, Faculty of Mechanical Engineering, Silesian University of Technology, 7 Towarowa St., 44-100 Gliwice, Poland
[b] Department of Engineering Materials and Biomaterials, Silesian University of Technology, 18a Konarskiego St., 44-100 Gliwice, Poland
[c] Department of Mining, Safety Engineering and Industrial Automation, Silesian University of Technology, 2 Akademicka St., 44-100 Gliwice, Poland
[d] Institute of Metallurgy and Materials Science of Polish Academy of Sciences, 25 Reymonta St., 30-059 Krakow, Poland

Article info

Article history:
Received 14 Jun. 2022
Received in revised form 01 Aug. 2022
Accepted 03 Aug. 2022
Available on-line 27 Sep. 2022

Keywords:
Antireflection coating; atomic layer deposition method; solar cells.

Abstract

Al_2O_3/TiO_2 thin films were deposited onto monocrystalline silicon surfaces using an atomic layer deposition. Their surface morphology and optical properties were examined for their possible use in solar cells. The surface condition and chemical composition were characterized using a scanning electron microscope and the thickness was measured using a spectroscopic reflectometer. The refractive index and the reflection characteristics were determined. First, the optical properties of the Al_2O_3 thin film and its influence on recombination in the semiconductor were examined. In this way, it can fulfil a double role in a solar cell. Since reflection reduction was only achieved in a narrow range, it was decided to use the Al_2O_3/TiO_2 system. Thanks to this solution, the light reflection was reduced in a wide range (even below 0.2%).

1. Introduction

An antireflection coating is a single layer, or a configuration of layers designed to minimize or completely eliminate the light reflection (glare) on optical elements. This reflection is created when the light passes through the boundaries of media with different refractive indices. At each medium boundary, both refraction and reflection of the incident light beam occur. While in the case of a lens, refraction is the most desirable phenomenon because it makes the authors' optical instrument work and reflection is what they would like to avoid. The reflected light from the centres border does not reach the authors' detector, causing a decrease in the effectiveness of the equipment [1–4].

In the case of an air-to-glass interface, 95% of the light passes through it and 5% is reflected. At first glance, it does not seem like much. However, if we consider that in a typical binocular the authors deal with 10–11 medium boundaries (lens consists of two connected lenses, two prisms, and an ocular), the losses are significant. It turns out that only 57% of the light falling on the lens passes through ordinary binoculars. In the case of photographic lenses, the situation can be even worse, because in complex zoom lenses, the number of lenses can be as high as 20.

Optical losses are also of great importance in the case of photovoltaic elements and devices. A bare silicon wafer (used in solar cells) reflects a lot of light. It is over 30%. The high reflectivity of polished silicon solar cells has given rise to the need for properly designed antireflection coatings to obtain improved efficiency. The reflection is reduced by developing surfaces and depositing optical thin layers on the front surface of solar cells. These optical thin films on silicon solar cells are similar to those used on other optical elements such as eyeglasses lenses [4–8].

The principle of antireflection coatings is based on the phenomenon of an electromagnetic wave interference. To achieve this effect with a single layer with a refractive index lower than the refractive index of the substrate, its optical thickness must be an odd multiple of λ/4. The reflected light goes out when the condition of dependence between the refractive indices for each optical environment is met:

$$\frac{n_0}{n_1} = \frac{n_1}{n_s}, \tag{1}$$

*Corresponding author at: marek.szindler@polsl.pl

https://doi.org/10.24425/opelre.2022.141952
1896-3757/ Association of Polish Electrical Engineers (SEP) and Polish Academic of Sciences (PAS). Published by PAS

where n_0, n_1, n_s are the refractive indices, successively: in the medium, in the thin film, and at the interface between the thin film and the substrate.

The thin film thickness is chosen so that the wavelength in the optical material is a quarter of the incident wavelength. For a quarter-wavelength thin film of a transparent material with the refractive index n_1 and light incident on the thin film with the free-space wavelength λ_0, the thickness d_1 which causes optimal reflection is computed by

$$d_1 = \frac{\lambda_0}{4n_1}. \quad (2)$$

Antireflection coatings used in silicon solar cells can be divided according to the number of layers on single-layer, double-layer, and multilayer antireflection coatings. A single-layer antireflection coating with a thickness of d_1 and the refractive index n_1 on a dielectric substrate with the refractive index n_s is shown schematically in Fig. 1 as an air-antireflection coating-substrate configuration. The light beam incident on a such configuration is partially reflected. The most common optical thin films used in photovoltaics are: TiO_2, SiO_2, SiN_x, a-SiNx:H, a-Si:C:H, ZnS, Ta_2O_5, Sn_xO_x, MgF_2 [8–12].

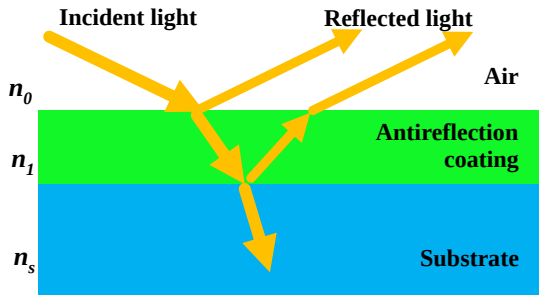

Fig. 1. Scheme of the influence of using a single antireflection coating on the light absorption.

The most used material in photovoltaics was titanium dioxide (TiO_2) with the refractive index equal to 2.58. The photoelectrochemical properties of TiO_2 are related to the absorption of radiation. The TiO_2 is defined by high absorption only in the ultraviolet range. In order to increase the extent of light absorption in the wider range, which is crucial in solar cells and in the degradation of water under the influence of light, work is continually being done to modify its properties. Silicon dioxide (SiO_2) is an inorganic compound with a crystalline structure and high hardness. In photovoltaics, SiO_2 is primarily used in the amorphous form with a refractive index of around 1.46. MgF_2 thin layers are also often used to coat the surface of optical elements with an antireflection coating. The refractive index of MgF_2 is equal to 1.38. A very popular antireflection coating used in photovoltaics in recent years is amorphous silicon nitride (a-SiNx) which works very well as a passivating layer for silicon and its refractive index is in the range of 1.7–2.3 [1, 2, 9].

Single-layer antireflection coatings are easy to fabricate and are used in many optical instruments. However, they have some limitations. For semiconductor substrates such as silicon, the reflection can only be extinguished in a narrow range after which the reflection increases drastically. The above limitations can be eliminated by using double-layer and multilayer antireflection coatings. The scheme of light reflection from a double-layer antireflection coating is shown in Fig. 2. Double-layer coatings create dielectric layers with thicknesses d_1, d_2, and refractive indices n_1, n_2 respectively, on a dielectric or semiconductor substrate with a refractive index n_s [12–16].

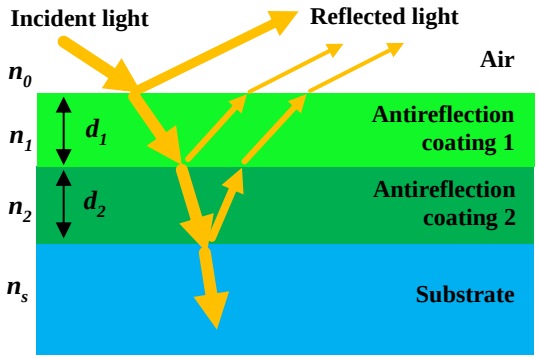

Fig. 2. Scheme of the influence of using a double antireflection coating on the light absorption.

Both devices and their elements are increasingly required to be multifunctional. It is similar with antireflection coatings. They are increasingly not only used to minimize reflection, but also to act as a passivating layer supporting electrical contacts or self-cleaning in silicon solar cells. The most popular configuration in solar cells was SiO_2/TiO_2 where SiO_2 and TiO_2 acted as a passivating and antireflection layer, respectively. Recently, Si_3N_4 and a-SiN_x layers, which can act as a passivating and antireflection layer simultaneously, have been increasingly used. The Al_2O_3/TiO_2 configuration is proposed in this article. Recombination is an undesirable phenomenon and occurs both on the surface and in the entire volume of the semiconductor at high speed. To slow down/prevent recombination, surface passivation is usually used with an SiO_2 layer. Replacing the SiO_2 layer with the Al_2O_3 layer will increase the short-circuit current in the solar cell and thus increase its efficiency [4]. Moreover, the Al_2O_3 layer, due to its properties, may also initially act as an antireflection coating. The atomic layer deposition (ALD) method was used in this article to deposit the proposed thin film configuration for silicon solar cells applications.

Figure 3 shows differences in the ability to cover an element with a developed surface for the most commonly used technologies. The physical vapour deposition (PVD) method covers only the surface of a component perpendicular to the stream. In the chemical vapour deposition (CVD) method, it is also possible to cover the surface parallel to the stream. In both cases, the so-called "coat" is obtained. The further away from the stream, the slower the deposition of the layer. Thus, there are variations in thickness. The opposite surface cannot be covered, as well. In the sol-gel method (solution deposition), the entire element can be covered, but the solution will partially or completely fill the developed surface. Therefore, a great advantage of the ALD method is the possibility of evenly covering the entire element in one process. In addition, the coating produced by this method imitates the shape of the surface, which is often useful, for example, when using a silicon solar cell on a textured surface. [2, 3, 5, 6].

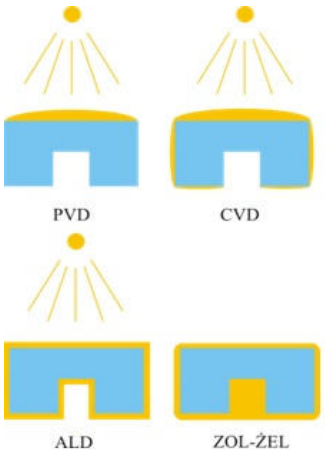

Fig. 3. Comparison of the ability to cover surfaces with complex shapes for different deposition methods.

2. Material descriptions and research methodology

Al_2O_3/TiO_2 double antireflection coatings were deposited using the ALD Picosun R 200 (Espoo, Finland) system. Trimethylaluminum (TMA) and H_2O were used as precursors for Al_2O_3 whereas titanium chloride (TiCl) and H_2O were used as the precursors for TiO_2. Typical thermal ALD parameters were used with a deposition temperature of 250°C with pulse lengths of 0.1 and 4 s forming precursor and water, respectively. An N_2 purge of 4 s was introduced between pulses to remove excess precursors and reaction by-products. Various combinations of the number of cycles of individual layers were changed. The number of cycles for individual Al_2O_3 and TiO_2 thin films was in the range of 100–1000.

First, ALD thin films were deposited on a polished silicon substrate (2 × 2 cm plates) with a low roughness coefficient to eliminate the influence of the substrate and characterize it well. Later in the experiment, thin films were deposited on a textured silicon wafer (2 × 2 cm plates). The surface of silicon wafers as a result of cutting during production is severely damaged. Therefore, the preparation of silicon wafers began with the removal of the damaged layer by bathing in a 20% KOH solution at 80 °C for 4 min. The plates were then immersed in a 1:1 volume ratio of 95% H_2SO_4:H_2O for 10 min to neutralize K^+ potassium and rinsed in a deionized water (DIH_2O) for 10 min. The next step was to perform the texture in an IPA + H_2O + KOH solution bath for 30 min which completed the stage of chemical treatment of silicon wafers. All samples (both polished and textured silicon) were subjected to the same cleaning procedure prior to deposition. They are placed in an ultrasonic scrubber, successively in detergent, isopropyl alcohol, and then in ethyl alcohol. In the final stage, they were placed in the plasma cleaner for 10 min.

The surface topography of the analysed samples was assessed by a scanning electron microscope (SEM). The pictures were taken with a Zeiss Supra 35 camera. The accelerating voltage was 3–5 kV. To obtain pictures of the surface morphology, the secondary electron detector (by the in-lens detector) was used. Qualitative studies of the chemical composition were also done using energy-dispersive spectrometry (EDS).

2D and 3D topographic images of 2 × 2 μm were taken using an XE-100 Park Systems atomic force microscope (AFM), and the root mean square (R_q) and roughness average (R_a) coefficient values were determined using an XEI software.

Thickness of the deposited layers was determined using an FR-pRo-UV/VIS spectroscopic reflectometer (ThetaMetrisis SA., Peristeri Greece). Measurements were taken in the reflectance mode. The total reflectance spectroscopy is the basis behind the reflectometer. This is the ratio of the intensity of the reflected light wave to the intensity of the incident light wave. The light beam by default incident on the surface of the sample, in turn, is reflected from top and bottom surfaces of the layer which is subjected to interference. Such beam is aimed through an optical fibre to a CCD matrix attached to a spectrometer via a computer. On the monitor, a spectrogram with rectilinear interference oscillations proportional to layer thickness can be seen.

The refractive index of the Al_2O_3 and TiO_2 layers was designated using an α spectroscopic ellipsometer (SE) from Woollam company (Lincoln, OR, USA).

The optical properties of the layers were examined using an UV-VIS 220 Evolution spectrophotometer from Thermo Fisher Scientific company (Waltham, MA, USA). The spectral range of the measurements was of 300–900 nm. Absolute reflection was estimated using an ISA-220 Integrating Sphere Accessory.

Changes in the short-circuit current (I_{sc}) on the entire silicon solar cell with an Al_2O_3 passivating layer were recorded using a Corescan device. A light-beam-induced current (LBIC) mode was used. The LBIC measurement mode involves scanning the whole surface of a silicon solar cell with a light beam and recording the changes of the short-circuit current for each position.

3. Results

SEM pictures were taken with a Zeiss Supra 35 camera setting an accelerating voltage from 3 kV to 25 kV. To obtain pictures of the surface morphology, a secondary electron (in-lens) detector was used because the substrate and the thin films are extremely flat. Therefore, high magnification (100 000 times and higher) was also required to see surface details. The surface morphology of thin films of Al_2O_3 and TiO_2 deposited directly one after another was examined. The topography of both layers deposited by ALD is homogeneous and flat (Fig. 4). The surface does not show any discontinuities, cracks, pores, and defects. The surface appearance of all the produced layers was very similar as the deposition conditions did not change, but only the number of cycles (thickness).

The chemical composition analysis of the prepared layer was analysed by the energy dispersive X-ray spectroscopy. In Fig. 5, the EDS spectra of ALD Al_2O_3/TiO_2 layers are shown. In the EDS spectra, peaks were recorded at about 0.452, 0.525, and 1.486 keV which are attributed to titanium, oxygen, and aluminium, respectively. Such an analysis proved the presence of aluminium oxide and titanium dioxide. Additionally, the peak of 1.739 eV was recorded, which comes from the silicon substrate. No other elements were registered indicating a clean process.

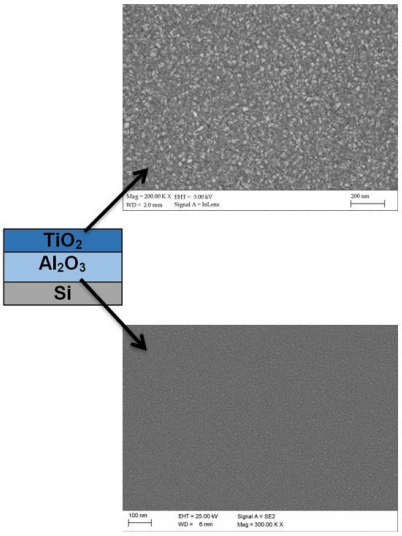

Fig. 4. Surface morphology of thin films of 30.15 nm Al_2O_3 and 36.21 nm TiO_2 deposited directly one after another.

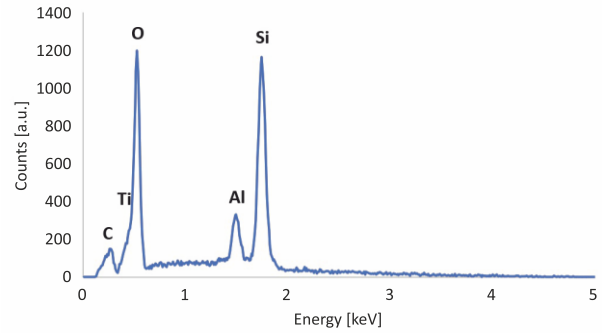

Fig. 5. EDS spectrum of thin films of 30.15 nm Al_2O_3 and 36.21 nm TiO_2 deposited directly one after another.

The surface morphology and its 3D representation of thin films of 30.15 nm Al_2O_3 and 36.21 nm TiO_2 deposited directly one after another were registered using an atomic force microscope (Fig. 6). It was found out that repetitive aggregations of atoms visible in the images have similar geometrical features, similar to an ellipsoid.

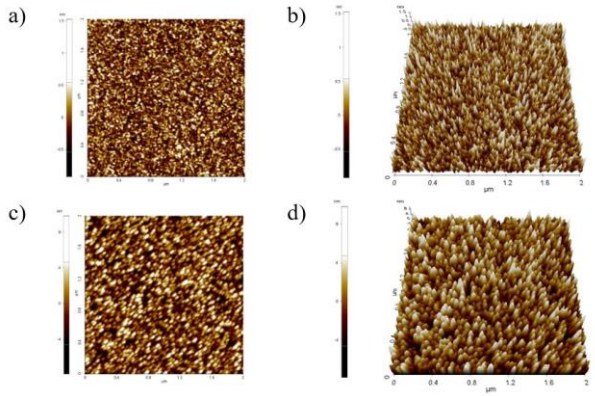

Fig. 6. AFM 2D and 3D images of the surface topography of thin films of 30.15 nm Al_2O_3 (a, b) and 36.21 nm TiO_2 (c, d) deposited directly one after another.

The Al_2O_3 thin film is characterized by a much lower roughness whose R_q and R_a parameters are equal to 0.28 and 0.22 nm, respectively. In turn, the TiO_2 thin film is characterized by a higher roughness whose parameters R_q and R_a are equal to 2.37 and 1.91 nm, respectively (Table 1).

Table 1.
Calculated values of the R_q and R_a of thin films of 30.15 nm Al_2O_3 and 36.21 nm TiO_2 deposited directly one after another.

Sample	R_q [nm]	R_a [nm]	Max. irregularity [nm]
30.15 nm Al_2O_3	0.28	0.22	1.52
36.21 nm TiO_2	2.37	1.91	3.26

In order to calculate the layer thickness, the light reflection in the range of 300–800 nm was measured. Figure 7 shows an exemplary experimental and fitted spectrum.

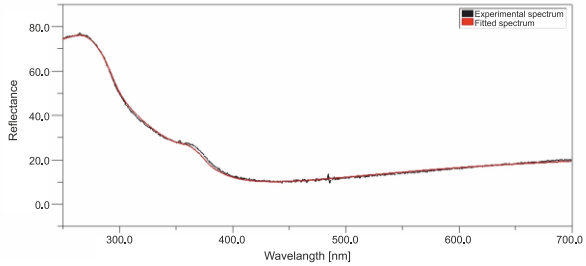

Fig. 7. Example of the experimental and fitted spectrum of thin films of 30.15 nm Al_2O_3 and 36.21 nm TiO_2 deposited directly one after another.

All measurements were characterized by a high fit factor. The parameter matching R^2 was always above 0.995. The thicknesses of the individual component layers are presented in Table 2.

Table 2.
The results of thickness measurements of individual layers.

Number of cycles	R^2	Al_2O_3 thickness [nm]	R^2	TiO_2 thickness [nm]
100	0.998	11.32	0.892	3.72
200	0.996	19.83	0.897	6.92
300	0.999	30.15	0.986	10.95
400	0.996	40.95	0.994	14.32
500	0.989	49.87	0.998	17.62
600	0.991	60.71	0.996	22.15
700	0.996	71.28	0.991	24.95
800	0.987	79.89	0.989	28.19
900	0.993	89.92	0.997	32.43
1000	0.998	100.53	0.999	36.21

The measurements were carried out for Al_2O_3 and TiO_2 thin films deposited with the number of cycles from 100 to 1000. From the determined thicknesses, it was possible to determine the average growth rate of a thin film during one ALD cycle. For aluminium oxide thin film, it is approximately 0.1 nm per cycle and for titanium oxide thin film, it is 0.035 nm per cycle. Samples of a double antireflection coating with different thicknesses of Al_2O_3 (100–1000 cycles) and TiO_2 (100–1000 cycles) individual layers were obtained.

The Cauchy and Lorenz models were used for the calculation of the refractive index and the extinction coefficient. In the measured range, the refractive index of the TiO_2 layer is in the range of 2.35–2.81, while the Al_2O_3 layer is in the range of 1.73–2.11 (Fig. 8).

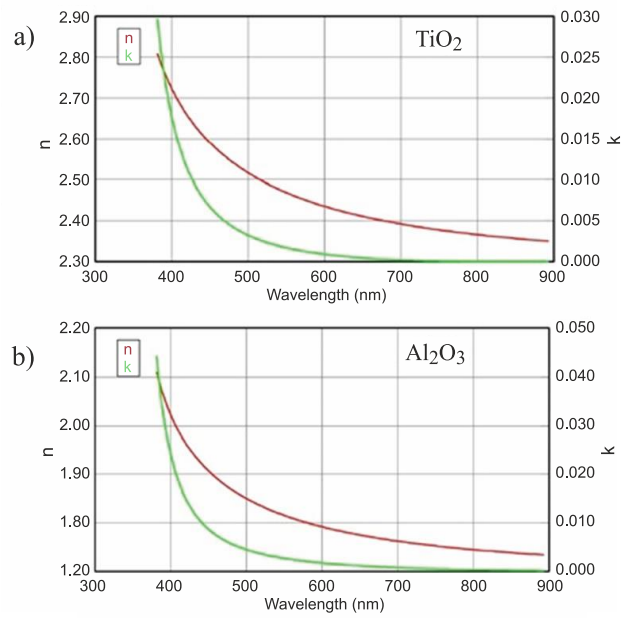

Fig. 8. Calculated refractive index and extinction coefficient using the Cauchy and Lorenz models for TiO_2 thin film (a) and Al_2O_3 thin film (b).

As it is reported in the literature that the Al_2O_3 thin film has good silicon passivating properties, it was decided to investigate its influence on the short-circuit current [17]. Deposition of a passivating thin film has a positive effect on the short-circuit current value. It can potentially replace SiO_2 in the SiO_2/TiO_2 system or replace the most used Si_3N_4. On the other hand, the TiO_2 thin film only plays an antireflection role, hence the research only in terms of minimizing light reflection. There was no need to measure the I_{sc} for this system. Since the Al_2O_3 thin film was like the bottom one, directly on the silicon, its influence on the passivation of the solar cell was investigated depending on thickness (Fig. 9). An increase in the value of the short-circuit current was recorded for a thickness up to about 30 nm and was equal to 59 mA. With further increase in thickness, the short-circuit current values were similar to each other. Therefore, when considering the bilayer system, the thickness of the Al_2O_3 layer will be approximately 30–40 nm as input value.

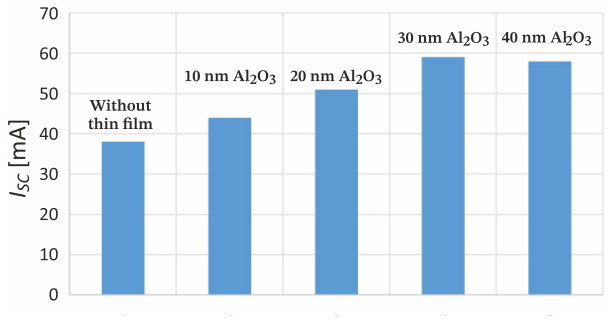

Fig. 9. Changes of short-circuit current I_{sc} in the prepared silicon solar cells registered by the LBIC method.

Since the aluminium oxide thin film works great as a passivating layer, it was decided to check its suitability as a single antireflection coating. According to (2), the optimal thin film thickness of about 90 nm was calculated. Such choice of thickness allows to minimize the reflection of light for a wavelength of 632.8 nm. The influence of the thickness of the aluminium oxide layer on the reflection from the surface of the polished silicon was also investigated. The reduction in thickness to about 60 nm shifts the minimum reflection to a shorter wavelength range (around 430 nm) (Fig. 10). On the other hand, the increase in thickness to about 120 nm shifts the minimum towards longer wavelengths (about 850 nm).

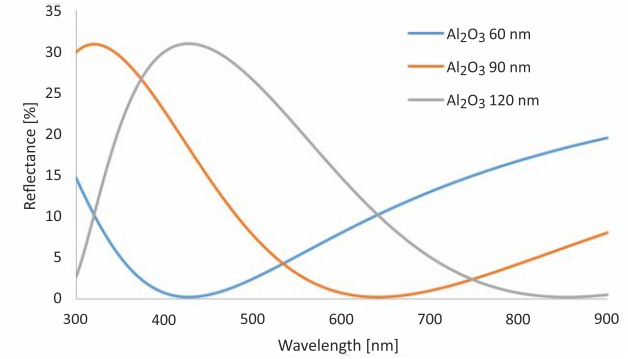

Fig. 10. Light reflection curve of polished silicon with deposited layers.

Figure 10 shows how to choose the thickness of an antireflection layer minimizing reflection in a narrow range. On the other hand, Figure 11 shows that when using a bilayer system, it is possible to select a layer that minimizes reflection in a wider range. A two-layer Al_2O_3/TiO_2 system was used to minimize the reflection of light in a wide range. The best results were obtained for the layer containing combinations of Al_2O_3 with a thickness of 30.15 nm (which resulted from the passivating properties) and TiO_2 with a thickness of 36.21 nm.

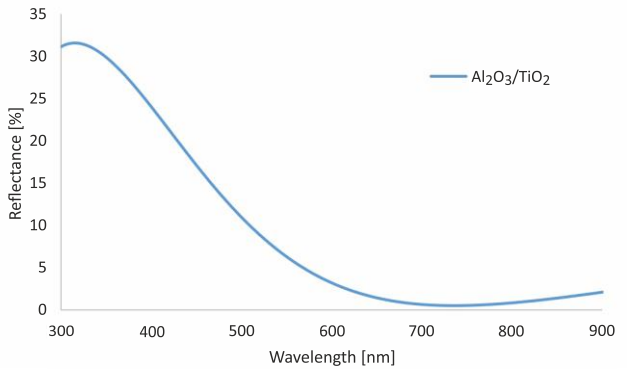

Fig. 11. Light reflection curve of polished silicon with deposited 30.15 nm Al_2O_3 and 36.21 nm TiO_2 double antireflection coating.

Electrochemically polished silicon substrate behaves like a mirror and reflects more than 90% of light. The use of an Al_2O_3/TiO_2 double antireflection coating made it possible to reduce the light reflection in the most important range for silicon solar cells (500–900 nm) below 10% (Fig. 10).

For a single Al_2O_3 layer, the reflection in the 550–900 nm range was significantly reduced. Outside of this range, however, the reflection grows sharply. On the other hand, for the Al_2O_3/TiO_2 system, it was possible to significantly reduce the reflection in the 550–900 nm range, and outside this range the reflection increases slower than in the first case.

It was checked how the deposited thin films together with the texture minimize the light reflection. For this purpose, the surface was developed by immersing a plate of monocrystalline silicon in an IPA + H_2O + KOH solution bath for 30 min. The resulting texture with a characteristic pyramidal shape was recorded using an atomic force microscope. The picture of the surface morphology was taken, and its 3D projection is shown in Fig. 12.

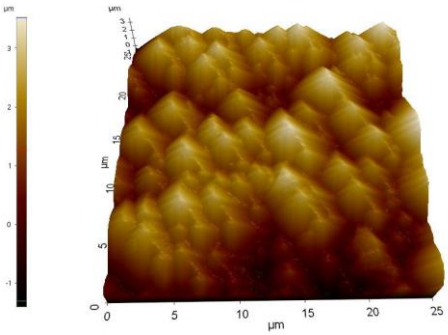

Fig. 12. 3D image of a 30.15 nm Al_2O_3 and 36.21 nm TiO_2 thin film deposited on a textured silicon substrate.

Such a procedure allows to minimize the light reflection below 10% in a wide range. The combination of the surface texturing stage and the deposition of the double antireflection coating allowed to minimize the light reflection in the 500–800 nm range even below 0.2% (Fig. 13). The best results were obtained for the layer containing Al_2O_3 with a thickness of 30.15 nm and TiO_2 with a thickness of 36.21 nm.

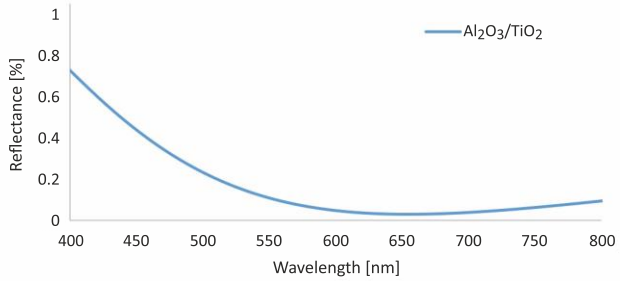

Fig. 13. Light reflection curve of textured silicon with deposited 30.15 nm Al_2O_3 and 36.21 nm TiO_2 double antireflection coating.

4. Conclusions

One of the requirements for thin films is their multi-functionality. It is not enough for the optical thin film to have only the desired spectral characteristics. They should also have other functions, e.g., passivating layers, increasing scratch resistance, self-cleaning, etc. Therefore, it was decided to use the Al_2O_3/TiO_2 double antireflection coating which enables both very good passivation of silicon and minimization of light reflection in the desired range for silicon. Thanks to such a layer, it was possible to increase the short-circuit current by more than 50% compared to a solar cell without a passivating layer. Moreover, the addition of a TiO_2 thin film allowed to minimize the reflection of light in a wide spectral range below 0.2%. Future research work will focus on the use of multi-layer coatings so that in the range of 300–500 it will also go below this value.

Authors' statement

Research concept and design, M. S.; collection and/or assembly of data, M. S., M. M. S., G. K. M; data analysis and interpretation, M. S., M. M. S., J. O.; writing the article, M. S.; critical revision of the article, M. S. and M. M. S.; final approval of article, M. S.

Acknowledgements

This publication was supported under the scholarship fund of the Silesian University of Technology in the field of scientific research and development works, 2022.

References

[1] Leon, J. J. D., Hiszpanski, A. M., Bond, T. C. & Kuntz, J. D. Design rules for tailoring antireflection properties of hierarchical optical structures. *Adv. Opt. Mater*. **5**, 1700080 1–8 (2017). https://doi.org/10.1002/adom.201700080

[2] Mousa, H. M., Shabat, M. M. & Karmoot, M. R. Double layer antireflection coating design for conductive solar cells. *Rom. Rep. Phys.* **72**, 416 (2020). http://rrp.infim.ro/2020/AN72416.pdf

[3] Drygała, A. *et al*. Influence of laser texturization surface and atomic layer deposition on optical properties of polycrystalline silicon. *Int. J. Hydrog. Energy* **41**, 7563–7567 (2016). https://doi.org/10.1016/j.ijhydene.2015.12.180

[4] Dobrzański, L. A., Szindler, M., Drygała, A. & Szindler, M. M. Silicon solar cells with Al_2O_3 antireflection coating. *Open Phys*. **12**, 666–670 (2014). https://doi.org/10.2478/s11534-014-0500-9

[5] Sarkar, S. & Pradhan, S. K. Silica-based antireflection coating by glancing angle deposition. *Surf. Eng*. **35**, 982–985 (2019). https://doi.org/10.1080/02670844.2019.1596578

[6] Szindler, M., Szindler, M. M., Boryło, P. & Jung, T. Structure and optical properties of TiO_2 thin films deposited by ALD method. *Open Phys*. **15**, 1067–1071 (2017). https://doi.org/10.1515/phys-2017-0137

[7] Dong, C. *et al*. Low emissivity double sides antireflection coatings for silicon wafer at infrared region. *J. Alloys Compd*. **742**, 729–735 (2018). https://doi.org/10.1016/j.jallcom.2018.01.384

[8] Boryło, P. *et al*. Structure and properties of Al_2O_3 thin films deposited by ALD proces. *Vacuum* **131**, 319–326 (2016). https://doi.org/10.1016/j.vacuum.2016.07.013

[9] Hou, G. J., Garcia, I. & Rey-Stolle, I. High-low refractive index stacks for broadband antireflection coatings for multijunction solar cells. *Sol. Energy* **217**, 29–39 (2021). https://doi.org/10.1016/j.solener.2021.01.060

[10] Sarkın, A. S., Ekren, N. & Saglam, S. A review of anti-reflection and self-cleaning coatings on photovoltaic panels. *Sol. Energy* **199**, 63–73 (2020). https://doi.org/10.1016/j.solener.2020.01.084

[11] Drabczyk, K., Kulesza-Matlak, G. & Drygała, A. Electro-luminescence imaging for determining the influence of metallization parameters for solar cell metal contacts. *Sol. Energy* **126**, 14–21 (2016). https://doi.org/10.1016/j.solener.2015.12.029

[12] Park, H. H. Inorganic materials by atomic layer deposition for perovskite solar cells. *Nanomaterials* **11**, 1–22 (2021). https://doi.org/10.3390/nano11010088

[13] Hossain, M. A. *et al*. Atomic layer deposition enabling higher efficiency solar cells: A review. *Nano Materials Sci.* **2**, 204–209 (2020). https://doi.org/10.1016/j.nanoms.2019.10.001

[14] Shanmugam, N. *et al*. Anti-reflective coating materials: a holistic review from pv perspective. *Energies* **13**, 2631 (2020). https://doi.org/10.3390/en13102631

[15] Zhang, W. *et al*. Broadband graded refractive index $TiO_2/Al_2O_3/MgF_2$ multilayer antireflection coating for high efficiency multi-junction solar cell. *Sol. Energy* **217**, 271–279 (2021). https://doi.org/10.1016/j.solener.2021.01.012

[16] Singh, R. *et al*.Growth of TiO_2 thin films on chemically textured Si for solar cell applications as a hole-blocking and antireflection layer. *Appl. Surf. Sci.* **418**, 225–231 (2017). https://doi.org/10.1016/j.apsusc.2017.01.307

[17] Suh D. Status of Al_2O_3/TiO_2-based antireflection and surface passivation for silicon solar cells. *Phys. Status Solidi Rapid Res. Lett.* **15**, 2100236 (2021). https://doi.org/10.1002/pssr.202100236